

Original Article



Interleukin-34 cancels anti-tumor immunity by PARP inhibitor

Takayoshi Nakamura ,^{1,2} Nabeel Kajihara ,¹ Naoki Hama ,¹
Takuto Kobayashi ,¹ Ryo Otsuka ,¹ Nanumi Han ,¹ Haruka Wada ,¹
Yoshinori Hasegawa ,³ Nao Suzuki ,² Ken-ichiro Seino ¹

¹Division of Immunobiology, Graduate School of Medicine, Institute for Genetic Medicine, Hokkaido University, Sapporo, Japan

²Department of Obstetrics and Gynecology, St. Marianna University School of Medicine, Kawasaki, Japan

³Department of Applied Genomics, Kazusa DNA Research Institute, Kisarazu, Japan

OPEN ACCESS

Received: Jun 23, 2022

Revised: Oct 5, 2022

Accepted: Nov 30, 2022

Published online: Dec 21, 2022

Correspondence to

Ken-ichiro Seino

Division of Immunobiology, Graduate School of Medicine, Institute for Genetic Medicine, Hokkaido University, Kita-15 Nishi-7, Sapporo, Hokkaido 060-0815, Japan.

Email: seino@igm.hokudai.ac.jp

© 2023. Asian Society of Gynecologic Oncology, Korean Society of Gynecologic Oncology, and Japan Society of Gynecologic Oncology

This is an Open Access article distributed under the terms of the Creative Commons Attribution Non-Commercial License (<https://creativecommons.org/licenses/by-nc/4.0/>) which permits unrestricted non-commercial use, distribution, and reproduction in any medium, provided the original work is properly cited.

ORCID iDs

Takayoshi Nakamura

<https://orcid.org/0000-0002-6968-2893>

Nabeel Kajihara

<https://orcid.org/0000-0003-0822-3391>

Naoki Hama

<https://orcid.org/0000-0003-4318-8448>

Takuto Kobayashi

<https://orcid.org/0000-0002-0096-6038>

Ryo Otsuka

<https://orcid.org/0000-0002-3730-9867>

Nanumi Han

<https://orcid.org/0000-0001-9524-1808>

ABSTRACT

Objective: Breast cancer susceptibility gene 1 (BRCA1)-associated ovarian cancer patients have been treated with a poly (ADP-ribose) polymerase (PARP) inhibitor, extending the progression-free survival; however, they finally acquire therapeutic resistance. Interleukin (IL)-34 has been reported as a poor prognostic factor in several cancers, including ovarian cancer, and it contributes to the therapeutic resistance of chemotherapies. IL-34 may affect the therapeutic effect of PARP inhibitor through the regulation of tumor microenvironment (TME).

Methods: In this study, The Cancer Genome Atlas (TCGA) data set was used to evaluate the prognosis of IL-34 and human ovarian serous carcinoma. We also used CRISPR-Cas9 genome editing technology in a mouse model to evaluate the efficacy of PARP inhibitor therapy in the presence or absence of IL-34.

Results: We found that *IL34* was an independent poor prognostic factor in ovarian serous carcinoma, and its high expression significantly shortens overall survival. Furthermore, in BRCA1-associated ovarian cancer, PARP inhibitor therapy contributes to anti-tumor immunity via the XCR1⁺ DC-CD8⁺ T cell axis, however, it is canceled by the presence of IL-34.

Conclusion: These results suggest that tumor-derived IL-34 benefits tumors by creating an immunosuppressive TME and conferring PARP inhibitor therapeutic resistance. Thus, we showed the pathological effect of IL-34 and the need for it as a therapeutic target in ovarian cancer.

Keywords: Interleukin-34; BRCA1-Associated Cancer; PARP Inhibitor; Therapeutic Resistance; XCR1⁺ Dendritic Cell; CD8⁺ T Cell

Synopsis

Interleukin (IL)-34 is an independent poor prognostic factor, and its high expression shortens overall survival in human ovarian serous carcinoma. When tumors express IL-34, poly (ADP-ribose) polymerase (PARP) inhibitor was not effective even in Brca1-deficient ovarian cancer. In the absence of IL-34, PARP inhibitors have anti-tumor immunity via the XCR1⁺ DC-CD8⁺ T cell axis.

Haruka Wada 
<https://orcid.org/0000-0002-5526-3647>

 Yoshinori Hasegawa 
<https://orcid.org/0000-0003-2904-6611>

 Nao Suzuki 
<https://orcid.org/0000-0002-7440-8127>

 Ken-ichiro Seino 
<https://orcid.org/0000-0003-4122-1718>

Conflict of Interest

No potential conflict of interest relevant to this article was reported.

Author Contributions

Conceptualization: N.T., K.N., H.N., O.R., H.N., W.H., S.N., S.K.I.; Data curation: N.T., K.N., K.T., O.R., H.Y.; Formal analysis: N.T., K.N., H.N., H.Y.; Funding acquisition: S.K.I.; Investigation: N.T.; Methodology: N.T., K.N., H.N., O.R., H.N., W.H., S.N., S.K.I.; Project administration: S.K.I.; Resources: S.K.I.; Software: N.T., K.T., H.Y.; Supervision: S.K.I.; Validation: O.R., H.N., W.H., S.N., S.K.I.; Writing - original draft: N.T., K.N.; Writing - review & editing: O.R., H.N., W.H., H.Y., S.N., S.K.I.

INTRODUCTION

Cellular deoxyribonucleic acid (DNA) can be exposed to exogenous and endogenous factors resulting in single- and double-strand breaks that could lead to detrimental consequences such as chromosomal aberrations, genomic instability, and cell death [1]. To prevent these events, cells equip a mechanism to activate poly (ADP-ribose) polymerase (PARP)-1, one of the DNA repair proteins, when DNA damage occurs [1]. PARP-1 contributes to intra-nuclear processes, including DNA repair, by catalyzing the protein's poly-ADP-ribosylation (PARylation) [1]. The reversible ADP-ribosylation of DNA by PARP-1 is responsible for an efficient DNA damage response [2]. In recent years, PARP inhibitor, which inhibits PARP-1 functions, has attracted attention as a novel therapeutic agent in epithelial ovarian and breast cancer [3,4]. PARP inhibitor was originally known as a medicine that triggered the synthetic lethal relationship between breast cancer susceptibility gene 1 and 2 (*BRCA1/2*) and PARP-1 in homologous recombination deficient (HRD), resulting in critical genomic instability and cell death [5]. However, later, it was revealed that PARP inhibitor traps PARP-1 at DNA replication forks and stabilizes the DNA-PARP-1 complex, resulting in replication fork collapse, finally leading to double-strand breaks and cell death [6].

PARP inhibitor has been shown to kill cancer cells by the mechanisms mentioned above and has also improved progression-free survival (PFS) in ovarian cancer [3]. Nevertheless, as well as other anti-cancer drugs, many patients treated with PARP inhibitor finally acquire therapeutic resistance [7]. Therefore, only a few reports show the prolongation of overall survival (OS) by PARP inhibitor therapy, and new therapeutic strategies such as combined use with immunotherapy are required to enhance the therapeutic effect of PAR inhibitor [7]. Indeed, PARP inhibitor increased programmed death-ligand 1 (PD-L1) expression on mouse ovarian and breast cancer cells, resulting in a synergistic anti-tumor effect when combined with anti-PD-L1 antibody [8,9]. Whereas, it has been reported that PARP inhibitor increased signal transducers and activators of transcription 3 (STAT3) activation in tumor and tumor-associated immune cells, promoting therapeutic resistance and immunosuppression [9]. Besides, tumor-associated macrophages (TAMs) infiltrating *BRCA1*-associated cancer tissue changed to immunosuppressive type by PARP inhibitor therapy, limiting its therapeutic effect [10]. Given these findings, manipulating the tumor microenvironment (TME) can improve the effects of anti-cancer drugs such as chemotherapeutic and immunotherapeutic agents [11].

The TME is a complex ecosystem of various cellular subsets, including tumor and immune cells, and changes dynamically during tumor progression [12]. When immunity works typically, cancer cells are taken up by antigen-presenting cells (APCs), and their information is presented to T cells, finally eliminated by CD8⁺ T cells [13]. However, in many stages of tumor formation, immunity falls to dysfunctional status via immunosuppressive cells such as regulatory T cells (Tregs), TAMs, and myeloid-derived suppressor cells (MDSCs), creating a favorable TME for tumor growth [14]. The representative factors that lead to the generation of immunosuppressive cells are tumor-derived inflammatory cytokines and chemokines, which potently suppress anti-tumor immunity in most cancer [11,15]. Interleukin (IL)-34, a pro-inflammatory cytokine, is locally expressed in the brain and skin under physiological conditions. Mouse IL-34 expression was also examined by single-cell RNA sequencing (scRNA-seq) in the whole mesentery and found to be expressed only in a subset of fibroblasts, endothelial cells, and mesothelial cells [16,17]. These reports indicated that no active IL-34 expression was found in the peritoneal cells under normal conditions, but its expression is increased in various diseases and is involved in cancer pathogenesis

[16,18]. In particular, it has been reported that IL-34 is an independent poor prognostic factor in breast cancer and colorectal cancer [18,19]. It has also been shown that high IL-34 expression in TME promotes tumor growth by mediating the induction and proliferation of immunosuppressive cells and hence contributes to the acquisition of therapeutic resistance to anticancer drugs [18].

Based on these backgrounds, in this study, we have investigated how IL-34 affects the therapeutic effect of PARP inhibitor via modulating TME. To investigate the antitumor efficacy of PARP inhibitors, we selected HM-1 and 4T1 cells in this study, which are high-grade tumors in mice. These cell lines were appropriate for our research because they are high-grade tumors with high cancerous and metastatic potential, rich in cytokine release, and frequently used in immunology studies [18,19]. Our results showed that IL-34 strongly limited the anti-tumor effect of PARP inhibitor in BRCA1-associated cancers via immunosuppressive changes in TME. On the other hand, IL-34 deficiency in cancer cells dramatically improved the anti-tumor effect of PARP inhibitor on murine BRCA1-associated ovarian cancers via a specific dendritic cell (DC)-CD8⁺ T cell axis. Here, we propose IL-34 as a responsible molecule of PARP inhibitor therapeutic resistance in BRCA1-associated cancers and suggest a novel therapeutic strategy.

MATERIALS AND METHODS

1. Cell lines

Mouse ovarian cancer cell line OV2944-HM-1 (HM-1) and breast cancer cell line 4T1 were purchased from the Japanese Collection of Research Bioresources and the American Type Culture Collection, respectively. The HM-1 and 4T1 cell lines were maintained in MEMa and RPMI-1640, respectively (Fujifilm Wako Pure Chemical Industries, Osaka, Japan). All culture media were supplemented with 10% fetal bovine serum (Sigma-Aldrich, St. Louis, MO, USA), 100 U/mL penicillin (Nacalai Tesque Inc., Kyoto, Japan), 100 µg/ml streptomycin (Nacalai Tesque Inc.), 0.1 mM MEM nonessential amino acids (Nacalai Tesque Inc.), and maintained at 37°C with 5% CO₂.

2. Generation of BRCA1 and IL-34 knockout (KO) cell line

BRCA1 and IL-34 KO HM-1 cell lines were generated using BRCA1 Double Nickase plasmid (#sc-419362-NIC; Santa Cruz Biotechnology, Dallas, TX, USA) or IL-34 Double Nickase plasmid (#sc-429354-NIC; Santa Cruz Biotechnology). The plasmids were transfected into 1×10⁵ cells per well using the TransIT-X2 (Mirus Bio, Madison, WI, USA) in a 6-well plate, and the cells were incubated for 48 hours. After incubation, successful transfection of the plasmid was visually confirmed by detecting green fluorescent protein (GFP) via fluorescent microscopy ObserverZ1 (Carl Zeiss AG, Oberkochen, Germany). Plasmid-transfected cells were selected by the GFP expression using FACSARIA™ II cell sorter (BD Biosciences, Franklin Lakes, NJ, USA) 48 hours after transfection. Then, puromycin (6 µg/mL) was added to the medium and cultured for 144 hours to select the transfected cells.

3. Protein expression analysis

Protein expression analysis for BRCA1 KO validation was performed by Western blotting. Cell lysates were obtained from each cell line by lysis in TNE buffer. The cell lysate was centrifuged to generate a supernatant sample. Protein concentrations of the supernatant samples were determined using the Pierce BCA™ Protein Assay Kit (#23225; Thermo Fisher

Scientific, Waltham, MA, USA). Supernatant samples were added to 6× sodium dodecyl sulfate (SDS) sample buffer containing 2-mercaptoethanol to achieve a total protein content of 40–50 µg per applied volume and were separated by electrophoretic migration at 200 V for approximately 40 minutes using a 10% acrylamide gel. Transcriptions were transferred to polyvinylidene difluoride (PVDF) membranes by the semidry method at 25 V for 30 minutes. The membrane was blocked with 3% skim milk for 1 hour at room temperature. The membrane was then probed with the BRCA1 antibody (287.17) (#sc-135732; Santa Cruz Biotechnology) at 4°C overnight with gentle shaking. It was also incubated with the corresponding horseradish peroxidase (HRP)-conjugated secondary antibody for 1 hour at room temperature. Proteins were visualized using Super Signal™ West Femto Maximum Sensitivity Substrate (#34094; Thermo Fisher Scientific).

4. DNA sequencing analysis

Genomic DNA sequencing analysis was performed to confirm the BRCA1 mutation in the cell lines. Genomic DNA was isolated from each cell line (1×10^6 cells) using 0.1% SDS-TNE buffer (10 mM Tris-HCl, 150 mM NaCl, 10 mM ethylenediaminetetraacetic acid [EDTA]). Polymerase chain reactions (PCRs) were performed using 1 µg of genomic DNA according to the Premix Ex Taq™ Hot Start Version (#RR030A; Takara Bio Inc., Kusatsu, Japan) manufacturer's instructions. The following primer pairs spanning the target sites were used in the PCR: *Brca1* (Forward: 5'-TGACGCCACCACCCTAGGC-3' and Reverse: 5'-TGTGCCCATTTTCGGACCTGCAT-3'). PCR products were purified using a 2% agarose gel and FastGene® Gel/PCR Extraction Kit (Nippon Genetics Co., Tokyo, Japan). Sanger sequencing was then performed. Purified PCR samples were prepared with BigDye® Terminator v3.1 Cycle Sequencing kit (Applied Biosystems, Waltham, MA, USA) and forward or reverse primers to a final dose of 20 µL and used for sequencing PCR. Samples were analyzed by ABI® PRISM 3130 Genetic Analyzer (Life Technologies, Carlsbad, CA, USA).

5. RNA sequencing analysis

Gene expression profiling and sequencing analysis were performed to confirm the major homologous recombination repair (HRR)-associated genes other than *Brca1* in the cell lines. RNA samples extracted from cells were transported to Kazusa DNA Research Institute (Kisarazu, Japan) for RNA sequence analysis. RNA samples were adjusted using the SureSelect Strand-Specific RNA library adjustment kit (G9691A; Agilent Technologies, Santa Clara, CA, USA) to the library, and these samples were used for sequencing by Illumina NextSeq500 (Illumina, Inc., San Diego, CA, USA). Mutation detection and annotation were performed using QIAGEN CLC Genomics Workbench (QIAGEN, Hilden, Germany). All detected mutation sites were checked against major HRR-associated gene sites other than *Brca1* to confirm the presence or absence of mutations, and changes in expression levels of those genes in *Brca1*^{KO} strains were examined. The major HRR-related genes were taken from the following references [20,21].

6. Cell proliferation assay

HM-1 and 4T1 cells (1×10^5) were seeded in 6 cm dishes. The number of cells (total cells including floating cells) was counted using a hemocytometer on day 3 or 4, and cells were seeded again after the count. These operations were repeated at least 6 times. Cell numbers were normalized and were relative to the number of cells seeded initially and were shown by the common logarithm. When the cells were counted, they were stained with trypan blue, and the blue-stained cells were excluded from the total cell count.

7. Cell viability assay

The cell viability of HM-1 and 4T1 cell lines was assessed by the 3-(4,5-dimethylthiazol-2-yl)-2,5-diphenyltetrazolium bromide (MTT) assay using MTT Cell Count Kit (Nacalai Tesque Inc.). Cells were seeded at a density of 2×10^3 in a 96-well plate and stimulated with some concentrations (0–5 μ M) of niraparib (MK-4827; AdooQ BioScience, Irvine, CA, USA), or 5×10^3 cells were stimulated with niraparib and some concentrations (0–50 μ M) of cisplatin. The cell viability was followed up to 3–4 days. Absorbance at a test wavelength of 570 nm and a reference wavelength of 650 nm was measured using a Multiskan™ FC (Thermo Fisher Scientific).

8. Gene expression analysis

Gene expression analysis was performed by quantitative PCR (qPCR). Total RNA was extracted using TRIsure reagent (Nippon Genetics Co.). Complementary DNA (cDNA) was synthesized from extracted RNA using ReverTra Ace qPCR RT Master Mix (Toyobo, Osaka, Japan). qPCR was performed on cDNA using KAPA SYBR® FAST qPCR Master Mix (2X) ABI Prism™ (Kapa Biosystems, Wilmington, MA, USA) on a StepOnePlus™ Real-Time PCR System (Thermo Fisher Scientific). The primers are listed in **Table S1**.

9. IL-34 quantification

The production of IL-34 from HM-1 and 4T1 cell lines was measured by the enzyme-linked immunosorbent assay (ELISA) using LEGEND MAX™ Mouse IL-34 ELISA Kit (Biolegend, San Diego, CA, USA). Cell culture supernatants were collected 48 hours after seeding the cells at a density of 1×10^6 in a 6 cm dish.

Protein was extracted from HM-1 Mock or *Brca1*^{KO} tumors and the concentration of IL-34 in each tumor was determined using an ELISA assay. For IL-34 expression analysis in tumors, 2×10^6 HM-1 cells were inoculated subcutaneously into the flank of syngeneic female mice. Tumors were collected when tumor size reached 10 mm in diameter. From the collected tumors, 10 mg of tumor tissue was weighed using a high-precision analytical balance (AND GH-202) and divided into 500 μ L of TNE buffer containing a protease inhibitor. Cell lysates were obtained from the measured tumor tissue which was crushed using a BioMasher® / PowerMasher II (Nippi, Inc., Tokyo, Japan) in TNE buffer. The cell lysate was centrifuged to generate a supernatant sample. Similarly, the concentration of IL-34 in the supernatant sample was determined by ELISA assay.

10. Mice experiments

Six to nine-week-old female B6C3F1 and BALB/c mice were purchased from Japan SLC or HOKUDO. The mice were maintained under specific pathogen-free conditions and housed in 12 hours light/12 hours dark cycle in the animal facility at Hokkaido University. For in vivo assay, 1×10^5 HM-1 or 4T1 cells were inoculated subcutaneously into the right flank of syngeneic female mice. Niraparib (5 mg/kg) was intraperitoneally administered when tumor size reached 5 mm in diameter. Tumor size was measured by caliper three times a week. The HM-1 and 4T1 tumors were collected 19 days after the cell inoculation. All animal procedures were approved by the Hokkaido University Animal Care Committee (approval number: 19-0094).

11. Isolation of tumor-infiltrating immune cells from solid tumor

Isolation of tumor-infiltrating immune cells from solid tumors was performed using BD Horizon™ Dri Tumor & Tissue (BD Biosciences). The recovered tumor-infiltrating cells were used as samples for flow cytometry.

12. Analysis of tumor-infiltrating immune cells

Tumor-infiltrating immune cells from solid tumors were analyzed by flow cytometry. Cells were washed and blocked with FcR Blocking Reagent (CD16/32; BioLegend) and stained with 4',6-diamidino-2-phenylindole (Cayman Chemical Company, Ann Arbor, MI, USA) and the antibodies against to following molecules; Cd3e, Cd4, Cd8a, Cd11b, Cd11c, Cd45, Cd69, Cd86, Cd206, F4/80, Gr-1, I-a/i-e, and Xcr1 (BioLegend). Data were acquired using FACSCelesta™ flow cytometer (BD Biosciences) and analyzed using FlowJo software.

13. FLT3L-driven DC differentiation of bone marrow cultures

Cell suspensions of mouse bone marrow were prepared by centrifugation of femurs, tibias and humerus with phosphate buffer saline followed by red blood cell lysis and filtering through a sterile 70 µm filter. The cells were suspended in D-MEM with L-Glutamine (Fujifilm Wako Pure Chemical Industries) supplemented with 10% fetal bovine serum, 100 U/mL penicillin, 100 µg/mL streptomycin, 0.1 mM MEM nonessential amino acids, 55 µM 2-mercaptoethanol and FLT3L 100 ng/mL (#550704; BioLegend) (DC medium). Cells were seeded at 8×10^6 cells per well in 4 mL of DC medium with 'IL-34 100 ng/mL (#577608; BioLegend) or nothing' and 'niraparib 2.5 µM or dimethyl sulfoxide (DMSO)' in 6-well plate and cultured at 37°C with 5% CO₂ for 9 days without replating medium.

14. Ovarian cancer bioinformatics analysis

From the ovarian serous carcinoma dataset (cBioPortal Ovarian Serous Cystadenocarcinoma—The Cancer Genome Atlas [TCGA], PanCancer Atlas; n=585), we used mRNA data files (276 patients with ovarian serous carcinoma) for survival analysis and excluded the other 309 patients because of incomplete RNA, OS, and PFS data. Data are classified as 'high' (138 patients) or 'low' (138 patients) bins at 50% (median) stringency thresholds for levels of gene expression, and Kaplan-Meier survival plot was generated.

15. Statistics

All statistical analysis was performed with JMP14 (SAS Institute, Cary, NC, USA). A two-sided Student's t-test was used to compare between 2 groups. Tukey's test was used to compare between 3 or more groups. On survival analysis, multivariate analysis was performed for OS using the Cox proportional hazards model. The Benjamin-Hochberg method was used to evaluate its superiority over the p-value after multiple comparisons. Kaplan-Meier survival plots were generated using JMP14 and evaluated using the log-rank test. The p-value was considered statistically significant when <0.05 .

RESULTS

1. PARP inhibitor did not suppress the BRCA1-associated tumor growth in vivo

PARP inhibitor has been used clinically in ovarian and breast cancers with HRD such as BRCA1 mutations [3,4]. There are various reports on acquiring therapeutic resistance to PARP inhibitor, but the mechanisms are still unclear [7]. In this study, we investigated the immunological aspects that may interfere with the efficacy of PARP inhibitor. To address this issue, we first established a murine BRCA1 KO ovarian cancer cell line (*Brcal*^{KO} HM-1) and confirmed knockout efficiency and indels by western blotting and sequencing analysis (**Fig. 1A, Fig. S1A-C**). Furthermore, the presence of mutations in major HRR-associated genes other than *Brcal* was examined using RNA sequence analysis, and no obvious mutations were found in these genes (**Table S2**). The established *Brcal*^{KO} HM-1 cell line, *in vitro*, showed equivalent

cell proliferation compared to the mock-transfected (Mock) HM-1 cell line and was sensitive to niraparib (one of the PARP inhibitor) or niraparib with cisplatin (Fig. 1B and C, Fig. S2A), and similar results were observed in murine BRCA1 KO breast cancer cell line (*Brca1*^{KO} 4T1) (Fig. S1D-F, Fig. S2B-D). This result is consistent with previous reports, suggesting that

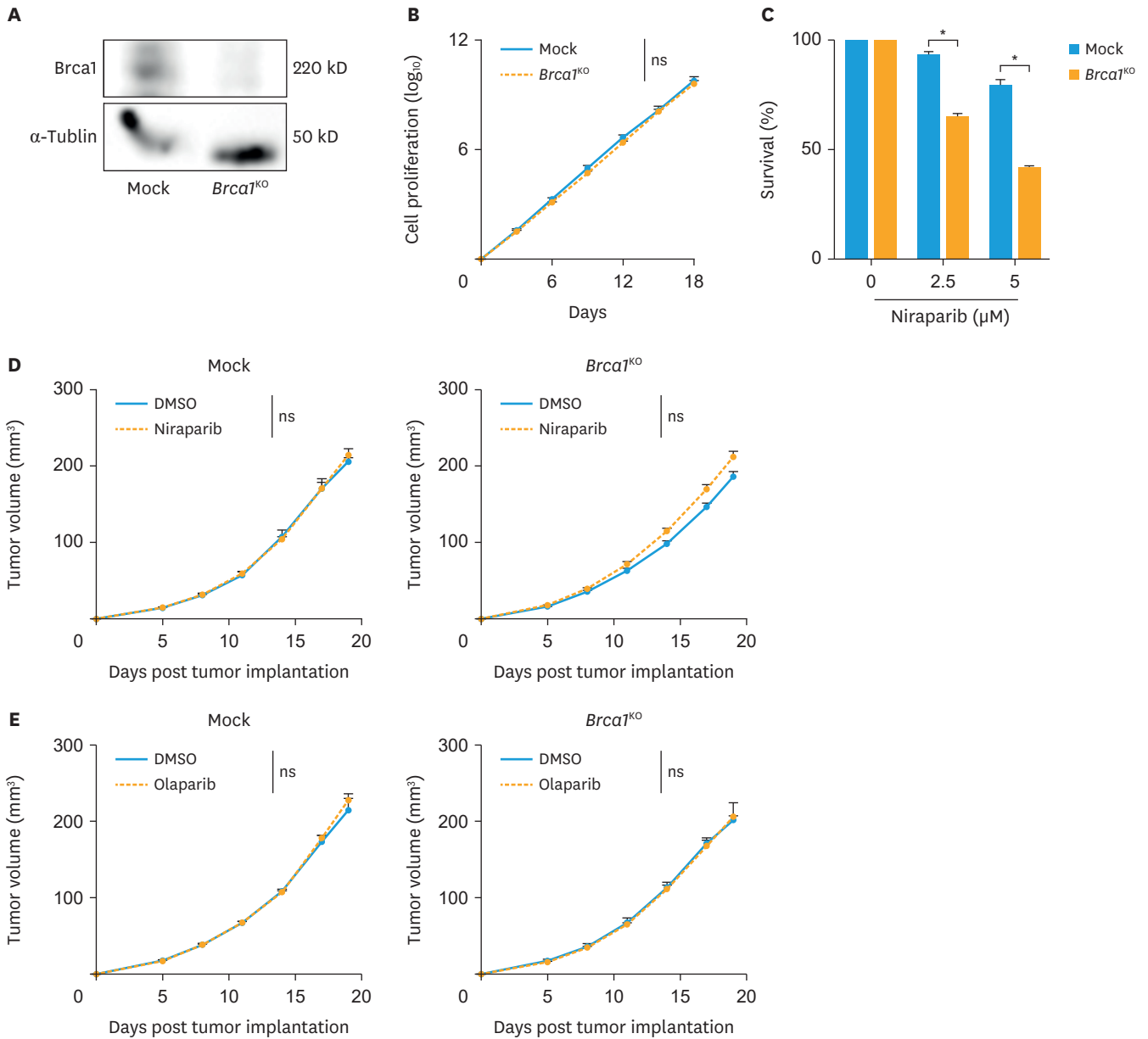


Fig. 1. PARP inhibition does not suppress the BRCA1-deficient ovarian cancer growth in vivo.

(A) Western blot of *Brca1* in Mock and *Brca1*^{KO} HM-1 cell lines. (B) The number of Mock and *Brca1*^{KO} HM-1 cells in cell culture was monitored at the indicated time points (n=3). (C) Cell viability (MTT assay) of Mock and *Brca1*^{KO} HM-1 cells treated with different concentrations of niraparib for 3 days (n=3). (D) Subcutaneous tumor growth of Mock and *Brca1*^{KO} HM-1 cells (1.0×10^5 cells, n=4 and n=6). Mice bearing Mock or *Brca1*^{KO} HM-1 tumors were treated daily with DMSO or niraparib (5 mg/kg, i.p.). (E) Subcutaneous tumor growth of Mock and *Brca1*^{KO} HM-1 cells (1.0×10^5 cells, n=4). Mice bearing Mock or *Brca1*^{KO} HM-1 tumors were treated daily with DMSO or olaparib (5 mg/kg, i.p.). (F) Inflammatory cytokine (*Il34*, *Il1b*, *Il6*, *Il17*, *Tnfa*, *Ifng*) expression of Mock and *Brca1*^{KO} HM-1 cells (1.0×10^6 cells, n=3) were determined by qPCR. (G) *Il34* expression levels of Mock and *Brca1*^{KO} HM-1 cells (1.0×10^6 cells, n=3) were determined by ELISA. (H) Mock or *Brca1*^{KO} HM-1 cells (1.0×10^5 cells, n=3) were transplanted subcutaneously into B6C3F1 mice. After 19 days of transplantation, tumor-infiltrating immune cells were isolated from tumors and subjected to flow cytometry analysis (n=3-4). Shown are percentages of Cd3e⁺, Cd11b⁺F4/80⁺MhcII⁺, and Cd11b⁺Gr-1⁺ within Cd45⁺ cells. BRCA, breast cancer susceptibility gene; DMSO, dimethyl sulfoxide; ELISA, enzyme-linked immunosorbent assay; IL, interleukin; i.p., intraperitoneally; MTT, 3-(4,5-dimethylthiazol-2-yl)-2,5-diphenyltetrazolium bromide; ns = not significant; PARP, poly (ADP-ribose) polymerase; qPCR, quantitative polymerase chain reaction. *p<0.05.

(continued to the next page)

IL-34 cancels antitumor immunity by PARP inhibitor

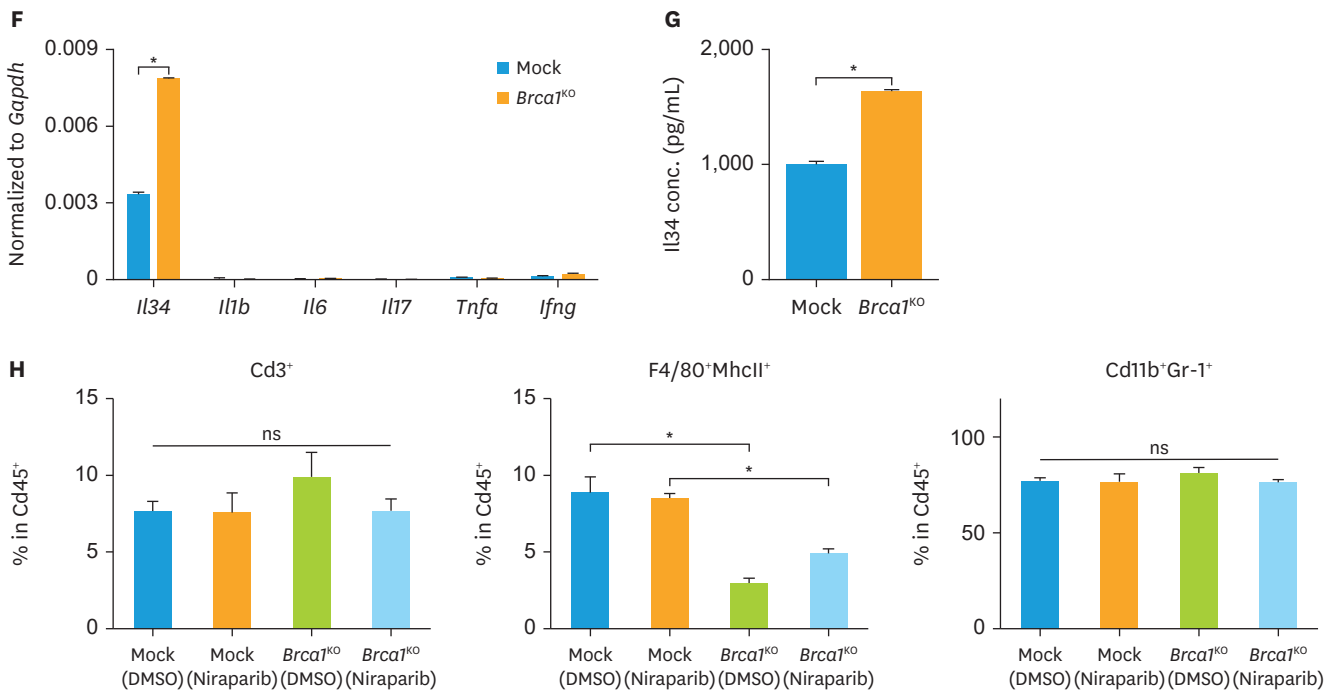


Fig. 1. (Continued) PARP inhibition does not suppress the BRCA1-deficient ovarian cancer growth in vivo. (A) Western blot of Brca1 in Mock and Brca1^{KO} HM-1 cell lines. (B) The number of Mock and Brca1^{KO} HM-1 cells in cell culture was monitored at the indicated time points (n=3). (C) Cell viability (MTT assay) of Mock and Brca1^{KO} HM-1 cells treated with different concentrations of niraparib for 3 days (n=3). (D) Subcutaneous tumor growth of Mock and Brca1^{KO} HM-1 cells (1.0×10⁵ cells, n=4 and n=6). Mice bearing Mock or Brca1^{KO} HM-1 tumors were treated daily with DMSO or niraparib (5 mg /kg, i.p.). (E) Subcutaneous tumor growth of Mock and Brca1^{KO} HM-1 cells (1.0×10⁵ cells, n=4). Mice bearing Mock or Brca1^{KO} HM-1 tumors were treated daily with DMSO or olaparib (5 mg /kg, i.p.). (F) Inflammatory cytokine (Il34, Il1b, Il6, Il17, Tnfa, Ifng) expression of Mock and Brca1^{KO} HM-1 cells (1.0×10⁶ cells, n=3) were determined by qPCR. (G) IL34 expression levels of Mock and Brca1^{KO} HM-1 cells (1.0×10⁶ cells, n=3) were determined by ELISA. (H) Mock or Brca1^{KO} HM-1 cells (1.0×10⁵ cells, n=3) were transplanted subcutaneously into B6C3F1 mice. After 19 days of transplantation, tumor-infiltrating immune cells were isolated from tumors and subjected to flow cytometry analysis (n=3–4). Shown are percentages of Cd3e⁺, Cd11b⁺F4/80⁺MhcII⁺, and Cd11b⁺Gr-1⁺ within Cd45⁺ cells. BRCA, breast cancer susceptibility gene; DMSO, dimethyl sulfoxide; ELISA, enzyme-linked immunosorbent assay; IL, interleukin; i.p., intraperitoneally; MTT, 3-(4,5-dimethylthiazol-2-yl)-2,5-diphenyltetrazolium bromide; ns = not significant; PARP, poly (ADP-ribose) polymerase; qPCR, quantitative polymerase chain reaction. *p<0.05.

Brca1^{KO} HM-1 cells cause HRD status due to loss of BRCA1, resulting in synthetic lethality by PARP inhibitor [5,6]. We then subcutaneously inoculated Mock and Brca1^{KO} HM-1 cells to mice and treated them with niraparib daily. Unexpectedly, in vivo, the administration of niraparib did not affect the growth of not only Mock but also Brca1^{KO} HM-1 tumors, and a similar result was obtained when we used 4T1 tumors (Fig. 1D, Fig. S3A). As yet another PARP inhibitor, we used olaparib, which was approved before niraparib and has been reported in many clinical and research studies, but again did not affect the growth of Brca1^{KO} HM-1 tumors (Fig. 1E). Based on several previous reports [11,22], we have predicted that changes in TME may have caused this phenomenon and analyzed the expression of several proinflammatory cytokines produced by Mock and Brca1^{KO} HM-1 cells. In both Mock and Brca1^{KO} HM-1 cells, while most inflammatory cytokines expressions were low, only IL-34 expression was substantially high; furthermore, IL-34 expressed significantly high in Brca1^{KO} HM-1 cells compared to Mock HM-1 cells (Fig. 1F and G). Further, we investigated intra-tumoral IL-34 expression in vivo. Similar to in vitro results of tumor cell lines, the expression of IL-34 was significantly increased in Brca1^{KO} HM-1 tumors (Fig. S3B). To determine how the differential expression of IL-34 alters each immune cell in TME, we evaluated tumor-infiltrating immune cells using flow cytometry. Mock and Brca1^{KO} HM-1 tumors did not show any change in T cell or MDSC populations regardless of niraparib administration and were maintained even with niraparib therapy, whereas MHCII⁺ macrophages notably decreased in Brca1^{KO} HM-1 tumors

compared to Mock HM-1 tumors and were maintained even with niraparib therapy (**Fig. 1H**). This result suggests that IL-34 suppressed the induction of activated-type macrophages. Collectively, these results suggest that even in BRCA1-associated cancers, the formation of immunosuppressive TMEs accompanied by high expression of IL-34 cancels the therapeutic effects of PARP inhibitor.

2. IL-34 expression canceled the anti-tumor effect of niraparib on BRCA1-associated cancer

From the previous chapter, since PARP inhibitor was not effective even in BRCA1-deficient tumors when tumors express IL-34, we first evaluated the clinical value of IL-34 in human ovarian serous carcinoma by using the TCGA dataset. Clinical data analysis revealed that *IL34* was a factor involved in the OS of ovarian serous carcinoma and was an independent prognostic factor (**Fig. 2A**, left, **Table 1**). Furthermore, supporting **Fig. 1H**, high *IL34* expression and low MHC class II expression in human ovarian serous carcinoma showed worse patient survival (**Fig. 2A**, right). Thus, targeting IL-34 could help to improve the clinical outcome of ovarian cancer patients. We next, to examine the relationship between IL-34 and therapeutic efficacy of PARP inhibitor therapy, established a murine BRCA1 and IL-34 KO ovarian cancer cell line (*Brca1^{KO}IL34^{KO}* HM-1), and confirmed IL-34 expression lost by ELISA assay (**Fig. S4A**). The established *Brca1^{KO}IL34^{KO}* HM-1 cell line, *in vitro*, showed equivalent cell proliferation compared to the *Brca1^{KO}* HM-1 cell line and was sensitive to niraparib, the same as the *Brca1^{KO}* HM-1 cell line (**Fig. S4B and C**). We then subcutaneously inoculated *Brca1^{KO}* and *Brca1^{KO}IL34^{KO}* HM-1 cells into mice and treated them with niraparib or olaparib daily. The administration of niraparib or olaparib suppressed the growth of *Brca1^{KO}IL34^{KO}* HM-1 tumors, and the niraparib anti-tumor effect was more drastic than we had imagined (**Fig. 2B**). We have predicted that changes in immune circumstances within TME may have caused this dramatic anti-tumor effect and then evaluated tumor-infiltrating immune cells in *Brca1^{KO}* and *Brca1^{KO}IL34^{KO}* HM-1 tumors. Notably, T cells were increased only in the *Brca1^{KO}IL34^{KO}* HM-1 tumors treated with niraparib, and the increment was primarily by activated-phenotype (**Fig. 2C**). This result suggests that the loss of IL-34 leads to the induction of CD8⁺ T cells by niraparib therapy, resulting in the creation of anti-tumor immune TME. In summary, these results indicate that *IL34* is a potent poor prognostic factor of ovarian serous cystadenocarcinoma in humans and that IL-34 expression suppresses the anti-tumor effect of PARP inhibitor therapy.

3. IL-34 cancels the cross-presenting DC-CD8⁺ T cell axis essential for PARP inhibitor therapeutic efficacy

To investigate the effect of CD4⁺ or CD8⁺ T cells on the anti-tumor effect of niraparib, *Brca1^{KO}IL34^{KO}* HM-1 tumors were treated with niraparib in mice pretreated with CD4- or

Table 1. Association of *IL34* and poor prognostic factors with overall survival

Gene	Exp (coefficient)	95% CI	p-value
<i>IL34</i>	4.1066	1.7437–9.6718	0.009
<i>OSBPL8</i>	2.8968	1.1747–7.1436	0.073
<i>LYPLA2</i>	2.2499	0.9264–5.4643	0.171
<i>EED</i>	1.8434	0.6460–5.2603	0.443
<i>MDM2</i>	1.6235	0.2923–9.0157	0.770
<i>IMPAD1</i>	1.5369	0.2266–10.4253	0.770
<i>CDC42</i>	0.9681	0.3599–2.6041	0.949

The data was obtained from the ovarian serous carcinoma dataset (276 patients with ovarian serous carcinoma). Survival analyses were performed using Cox proportional hazards modeling. p-values are used to assess significance after adjusting for multiple comparisons using the Benjamini-Hochberg method. CI, confidence interval.

IL-34 cancels antitumor immunity by PARP inhibitor

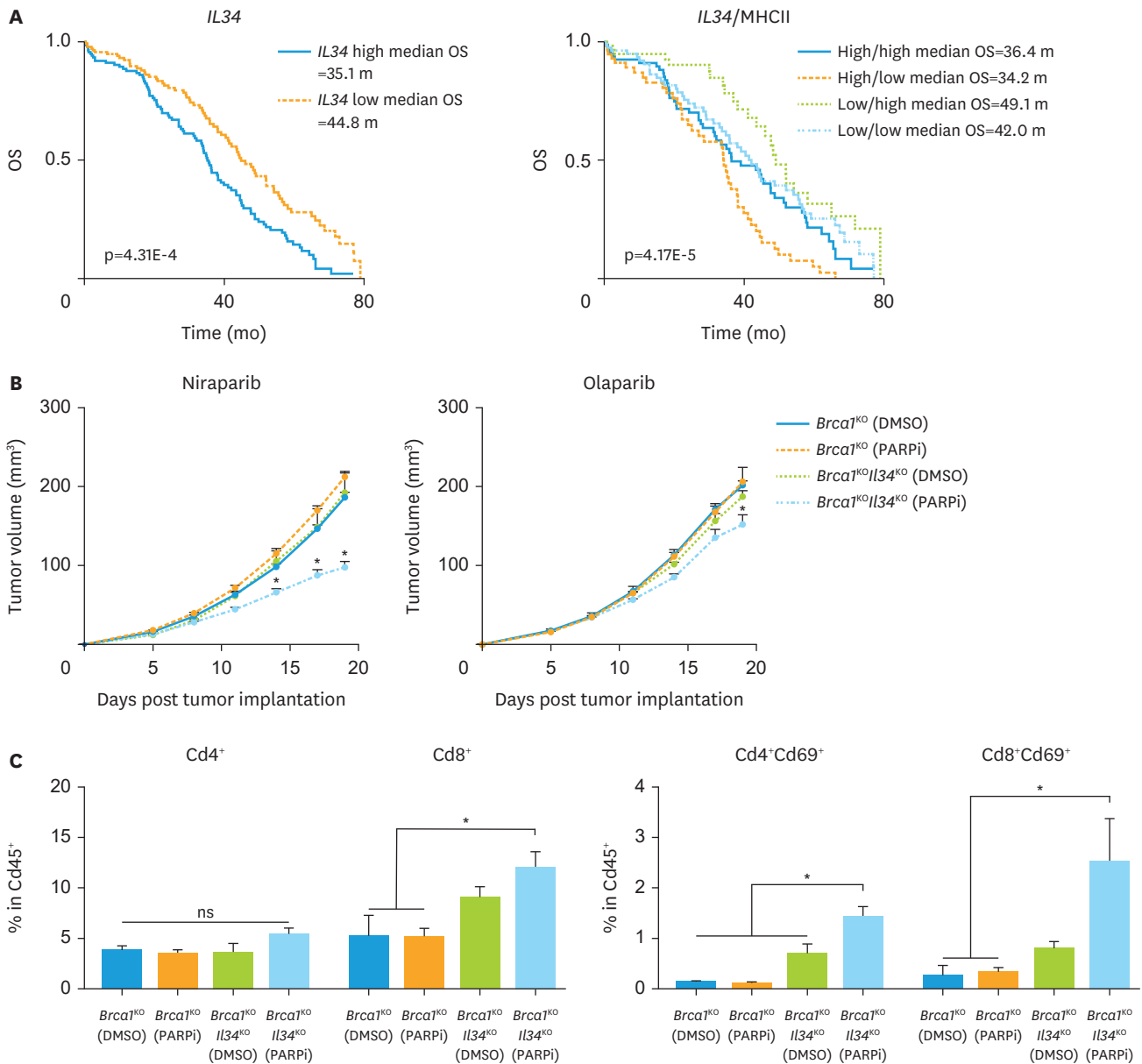


Fig. 2. PARP inhibition suppresses the BRCA1- and IL-34-deficient ovarian cancer growth in vivo. (A) Kaplan-Meier plot for OS of patients with ovarian serous carcinoma median split for the gene expression of *IL34* and the combination with MHCII. The patients were classified as IL-34 “high” (n=138) or “low” (n=138) in left figure, and as IL-34 and MHCII “high/high” (n=80), “high/low” (n=58), “low/high” (n=58) or “low/low” (n=80) in right figure. (B) Subcutaneous tumor growth of *Brca1*^{KO} and *Brca1*^{KO}/*IL34*^{KO} HM-1 cells treated with niraparib or olaparib (1.0×10⁵ cells, niraparib group n=6 and n=9, olaparib group n=4 and n=8). Mice bearing *Brca1*^{KO} or *Brca1*^{KO}/*IL34*^{KO} HM-1 tumors were treated daily with DMSO or PARP inhibitor (5 mg /kg, i.p.). (C) *Brca1*^{KO} or *Brca1*^{KO}/*IL34*^{KO} HM-1 cells (1.0×10⁵ cells, n=3) were transplanted subcutaneously into B6C3F1 mice. After 19 days of transplantation, tumor-infiltrating immune cells were isolated from tumors and subjected to flow cytometry analysis (n=3). Shown are percentages of Cd3e⁺Cd4⁺, Cd3e⁺Cd8a⁺, Cd3e⁺Cd4⁺Cd69⁺, and Cd3e⁺Cd8a⁺Cd69⁺ within Cd45⁺ cells. BRCA, breast cancer susceptibility gene; DMSO, dimethyl sulfoxide; IL, interleukin; i.p., intraperitoneally; OS, overall survival; ns = not significant; PARP, poly (ADP-ribose) polymerase. *p<0.05.

CD8-depleting antibodies. Mice lacking CD8⁺ T cells lost the anti-tumor effect of niraparib therapy on *Brca1*^{KO}/*IL34*^{KO} HM-1 tumors. On the other hand, mice lacking CD4⁺ T cells showed no loss of anti-tumor effect of niraparib therapy (Fig. 3A). These results clearly indicate that CD8⁺ T cells are essential for the anti-tumor effect of niraparib and that CD4⁺ T cells are not involved. Recently, the presence of DCs that directly cross-present CD8⁺ T cells without CD4⁺

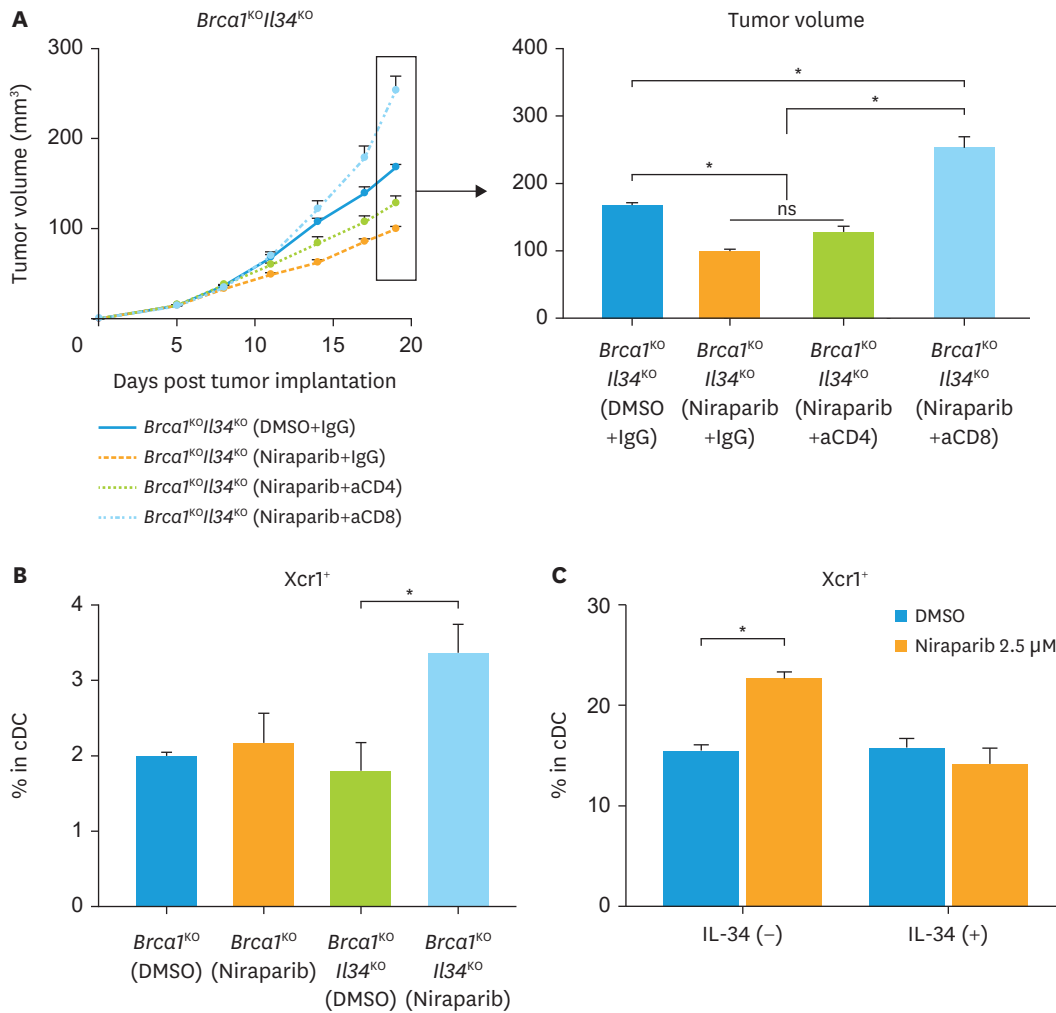


Fig. 3. PARP inhibition activates CD8⁺ T cells in a specialized dendritic cell-mediated system, resulting in antitumor effects. (A) Subcutaneous tumor growth of *Brca1^{KO}Il34^{KO}* HM-1 cells (1.0×10^5 cells, $n=3$). Mice were treated with anti-CD4 or anti-CD8 antibodies before 6 or 1 day of tumor cell transplantation. Mice bearing *Brca1^{KO}Il34^{KO}* HM-1 tumors were treated daily with DMSO or niraparib (5 mg/kg, i.p.). (B) *Brca1^{KO}* or *Brca1^{KO}Il34^{KO}* HM-1 cells (1.0×10^5 cells, $n=3$) were transplanted subcutaneously into B6C3F1 mice. After 19 days of transplantation, tumor-infiltrating immune cells were isolated from tumors and subjected to flow cytometry analysis ($n=3$). Shown are percentages of Xcr1⁺ within Cd45⁺Cd11b⁺F4/80⁺MhcII⁺Cd11c⁺ cells. (C) The subset composition of differentiated bone marrow cells. Bone marrow cells were induced to differentiate in vitro by the presence of FLT3L with 'IL-34 or nothing' and 'niraparib or DMSO'. Shown are percentages of Xcr1⁺ within Cd45⁺Cd11b⁺F4/80⁺MhcII⁺Cd11c⁺ cells. cDC, conventional dendritic cell; DMSO, dimethyl sulfoxide; IgG, immunoglobulin G; IL, interleukin; ns = not significant; PARP, poly (ADP-ribose) polymerase. * $p < 0.05$.

T cells have attracted attention in anti-tumor immunity, so we further investigated tumor-infiltrating DCs [23]. Interestingly, only in *Brca1^{KO}Il34^{KO}* HM-1 tumors treated with niraparib the percentage of XCR1⁺ DC was increased (Fig. 3B), suggesting that the cross-presenting DC-CD8⁺ T cell axis may be necessary for the anti-tumor effect of PARP inhibitor therapy. To investigate whether the presence of IL-34 is responsible for the decrease in XCR1⁺ DC, DCs were induced from mouse bone marrow cells to differentiate in the presence and absence of IL-34 and niraparib. In the absence of IL-34, niraparib therapy promoted induction of XCR1⁺ DC, whereas it was canceled in the presence of IL-34 (Fig. 3C). These results suggest that the formation of anti-tumor immune TME via activation of the XCR1⁺ DC-CD8⁺ T cell axis is essential for the anti-tumor effect of PARP inhibitor therapy, but the presence of IL-34 strongly suppresses it.

DISCUSSION

Cancer cells constantly promote the acquisition of therapeutic resistance by creating immunosuppressive TME [11,14]. Unfortunately, a critical factor in acquiring resistance to various chemotherapies, including PARP inhibitor therapy, is still unknown [7]. The present data showed for the first time that the XCR1⁺ DC-CD8⁺ T cell axis is crucial for the antitumor effect of PARP inhibitor therapy, and tumor-derived IL-34 can suppress this effect in ovarian cancer. In this section, we explain the value of IL-34 in therapeutic resistance and the rationale of IL-34-targeted therapy.

IL-34 is a cytokine that contributes to myeloid cell differentiation and proliferation and is implicated in various diseases, including cancer [18,19]. Indeed, tumor-derived IL-34 contributes to the survival of the tumors themselves through autocrine pathways; on the other hand, it induces the differentiation and recruiting of immunosuppressive TAMs and MDSCs through paracrine pathways [18,19]. Furthermore, it has been reported that tumor-derived IL-34 expression is enhanced when cancer cells' survival is threatened by chemotherapy [24]. High IL-34 expression enhances cytokine production, such as IL-6 and IL-10, by activating STAT3 and nuclear factor- κ B (NF- κ B) signaling pathways, resulting in strong support for the creation of immunosuppressive TME [25]. Notably, IL-34 expression in ovarian cancer was enhanced by chemotherapy, and its high expression shortened PFS [26]. In this study, TCGA dataset analysis revealed that IL-34 is an independent poor prognostic factor in ovarian serous carcinoma, and its high expression shortens OS. Although PARP inhibitor therapy has been indicated in ovarian cancer patients with *BRCA1* mutations [3], interestingly, *Brca1*-deficient tumors were not responsive to PARP inhibitor therapy in the murine ovarian cancer model. To investigate the cause of this unexpected result, we screened cytokines secreted from the mouse ovarian cancer used in this study and found that IL-34 was dramatically highly expressed. The absence of functional *BRCA1* in tumors has been shown to activate the NF- κ B pathway due to increased reactive oxygen species (ROS) [27]. Furthermore, it has been reported that IL-34 expression is upregulated upon NF- κ B activation due to cellular stresses, such as chemotherapeutic agents [24]. Namely, it suggested that activation of the NF- κ B pathway by loss or mutation of *BRCA1* could increase IL-34 expression. Thereby, we hypothesized that IL-34 caused resistance to PARP inhibitor therapy and examined this question. To this end, we disrupted IL-34 from *Brca1*-deficient tumors, PARP inhibitor therapy showed a marked antitumor effect by increasing activated CD8⁺ T cells within TME. Accumulating evidence indicated that, in *BRCA1*-associated ovarian cancer, enhancement of CD8⁺ T cells via activation of the STING pathway is essential for the antitumor effect of PARP inhibitor therapy [28]. Generally, to present antigens from APCs to T cells, endogenous antigens are presented to CD8⁺ T cells by APCs' MHC class I and exogenous antigens are presented to CD4⁺ T cells by APCs' MHC class II [13]. Although tumor antigen-specific CD4⁺ T cells are known to assist in the activation and proliferation of CD8⁺ T cells, thereby enhancing the anti-tumor effect, our data indicate that but not CD4⁺ T cells, CD8⁺ T cells are essential for the anti-tumor effect of PARP inhibitor therapy. Therefore, we assumed the involvement of cells that can present antigen directly to CD8⁺ T cells.

The cross-presenting DCs can efficiently present exogenous antigens directly to CD8⁺ T cells via the MHC class I pathway [23,28,29]. Our data showed that an increase in XCR1⁺ DC contributes to an increase in activated CD8⁺ T cells in PARP inhibitor therapy for ovarian cancer resulting in an anti-tumor effect. Many reports are indicating the importance of this interrelationship in anti-tumor immunity. In ovarian cancer, it has been reported that tumor-infiltrating DCs, including cross-presenting DCs, positively correlate with clinical outcomes [30]. Similarly, in melanoma,

the amount of intra-tumoral cross-presenting conventional DCs (cDCs) correlated with OS [31]. In addition, cross-presenting cDCs were positively correlated with survival in breast cancer, squamous cell carcinoma of the head and neck, and lung cancer [32]. Thus, this report can be one of the base studies that will boost therapies targeting the XCR1⁺ DC-CD8⁺ T cell axis.

Tumor-infiltrating immune cells receive a variety of homeostatic inhibitory stimuli from TME. For instance, IL-6, which abound in most cancer's TME, can reprogram precursor DCs (pre-DCs) into immunosuppressive DCs [33]. Indeed, it has been evident that DCs' functional maturation is strongly inhibited by a positive feedback loop in the STAT3/NF- κ B/IL-6 pathway [34]. PARP inhibitor therapy promotes type I interferon (IFN) production via the cGAS-STING pathway and the type I IFN signaling is required for the activation of cDCs [28,35]. However, it has also recently been reported that PARP inhibitor therapy promotes STAT3 activation in tumor-infiltrating immune cells in ovarian cancer [36]. It suggests that cDCs differentiation may be inhibited. Most notably, as mentioned above, given that IL-34 enhances cytokine production such as IL-6 and IL-10 via the STAT3/NF- κ B signaling pathway [18,25], PARP inhibitor therapy constantly suppresses immune cells' activation in presence of IL-34. Our data demonstrated that IL-34 inhibited differentiation into XCR1⁺ DCs and robustly suppressed anti-tumor immunity during PARP inhibitor therapy in ovarian cancer. Namely, it considers that IL-34 forcibly suppressed XCR1⁺ DCs' inducing via over-enhancing STAT3/NF- κ B/IL-6 pathway during PARP inhibitor therapy.

Three general mechanisms of acquired resistance to PARP inhibitor have been already known [7]: 1) Drug target-related effects; the upregulation of the drug efflux transporter ABCB1 [37], or mutations in PARP1 that either reduce the affinity of the PARP inhibitor or preserve endogenous functions of the enzyme when bound to a PARP inhibitor [38]; 2) Restoration of HR owing to restoration of BRCA1/2 function or functionally related proteins; such as reversion mutations or epigenetic alterations that induce the re-expression of a BRCA1 or BRCA2 wild-type protein or result in hypomorphic variants [39]; 3) Loss of DNA end-protection and/or restoration of replication fork stability; such as depletion of the MLL3/4 complex protein PTIP or the nucleosome remodeling factor CHD4, resulting in fork protection and resistance to PARP inhibitor in BRCA1/2-deficient cells [40]. However, there have been no previous reports of tumor immunity, particularly IL-34, acting on PARP inhibitor resistance. In this study, we revealed a novel mechanism of resistance against PARP inhibitor in which TME is regulated by tumor-derived IL-34. It is possible that IL-34-mediated immunosuppression and the previously described mechanisms work additively or synergistically to produce overall resistance. Further studies are required to elucidate this issue. Further studies would also clarify the mechanism of PARP inhibitor therapy-induced XCR1⁺ DC increment and whether IL-34 has negative effects on PARP inhibitor, such as inhibiting or suppressing synthetic lethality or PARP-trapping effects. IL-34 benefits tumors through various roles and may be a biomarker for therapeutic resistance and a worse prognosis. In addition, targeting IL-34 for therapy may be beneficial for restoring chemotherapeutic resistance and increasing sensitivity to immune checkpoint blockade therapy.

SUPPLEMENTARY MATERIALS

Table S1

Primer list for qPCR analysis

[Click here to view](#)

Table S2

Major HRR-associated gene expression profiling of wild type and *Brca1*^{KO} HM-1 cells

[Click here to view](#)

Fig. S1

Sequence trace views of mouse ovarian cancer and breast cancer cell.

[Click here to view](#)

Fig. S2

The effect of PARP inhibition on BRCA1-deficient cancer in vitro.

[Click here to view](#)

Fig. S3

The effect of PARP inhibition on BRCA1-deficient breast cancer growth in vivo.

[Click here to view](#)

Fig. S4

The effect of PARP inhibition on BRCA1- and IL-34-deficient ovarian cancer in vitro.

[Click here to view](#)

REFERENCES

1. Ray Chaudhuri A, Nussenzweig A. The multifaceted roles of PARP1 in DNA repair and chromatin remodelling. *Nat Rev Mol Cell Biol* 2017;18:610-21.
[PUBMED](#) | [CROSSREF](#)
2. Talhaoui I, Lebedeva NA, Zarkovic G, Saint-Pierre C, Kutuzov MM, Sukhanova MV, et al. Poly(ADP-ribose) polymerases covalently modify strand break termini in DNA fragments in vitro. *Nucleic Acids Res* 2016;44:9279-95.
[PUBMED](#) | [CROSSREF](#)
3. Pujade-Lauraine E, Ledermann JA, Selle F, Gebski V, Penson RT, Oza AM, et al. Olaparib tablets as maintenance therapy in patients with platinum-sensitive, relapsed ovarian cancer and a BRCA1/2 mutation (SOLO2/ENGOT-Ov21): a double-blind, randomised, placebo-controlled, phase 3 trial. *Lancet Oncol* 2017;18:1274-84.
[PUBMED](#) | [CROSSREF](#)
4. Cortesi L, Rugo HS, Jackisch C. An overview of PARP inhibitors for the treatment of breast cancer. *Target Oncol* 2021;16:255-82.
[PUBMED](#) | [CROSSREF](#)
5. Farmer H, McCabe N, Lord CJ, Tutt AN, Johnson DA, Richardson TB, et al. Targeting the DNA repair defect in BRCA mutant cells as a therapeutic strategy. *Nature* 2005;434:917-21.
[PUBMED](#) | [CROSSREF](#)
6. Murai J, Huang SY, Das BB, Renaud A, Zhang Y, Doroshow JH, et al. Trapping of PARP1 and PARP2 by clinical PARP inhibitors. *Cancer Res* 2012;72:5588-99.
[PUBMED](#) | [CROSSREF](#)
7. Dias MP, Moser SC, Ganesan S, Jonkers J. Understanding and overcoming resistance to PARP inhibitors in cancer therapy. *Nat Rev Clin Oncol* 2021;18:773-91.
[PUBMED](#) | [CROSSREF](#)

8. Jiao S, Xia W, Yamaguchi H, Wei Y, Chen MK, Hsu JM, et al. PARP inhibitor upregulates PD-L1 expression and enhances cancer-associated immunosuppression. *Clin Cancer Res* 2017;23:3711-20.
[PUBMED](#) | [CROSSREF](#)
9. Ding L, Chen X, Xu X, Qian Y, Liang G, Yao F, et al. PARP1 suppresses the transcription of PD-L1 by poly(ADP-ribose)ylating STAT3. *Cancer Immunol Res* 2019;7:136-49.
[PUBMED](#) | [CROSSREF](#)
10. Mehta AK, Cheney EM, Hartl CA, Pantelidou C, Oliwa M, Castrillon JA, et al. Targeting immunosuppressive macrophages overcomes PARP inhibitor resistance in BRCA1-associated triple-negative breast cancer. *Nat Can* 2021;2:66-82.
[PUBMED](#) | [CROSSREF](#)
11. Pitt JM, Marabelle A, Eggermont A, Soria JC, Kroemer G, Zitvogel L. Targeting the tumor microenvironment: removing obstruction to anticancer immune responses and immunotherapy. *Ann Oncol* 2016;27:1482-92.
[PUBMED](#) | [CROSSREF](#)
12. Zahir N, Sun R, Gallahan D, Gatenby RA, Curtis C. Characterizing the ecological and evolutionary dynamics of cancer. *Nat Genet* 2020;52:759-67.
[PUBMED](#) | [CROSSREF](#)
13. Bos R, Sherman LA. CD4+ T-cell help in the tumor milieu is required for recruitment and cytolytic function of CD8+ T lymphocytes. *Cancer Res* 2010;70:8368-77.
[PUBMED](#) | [CROSSREF](#)
14. Munn DH, Bronte V. Immune suppressive mechanisms in the tumor microenvironment. *Curr Opin Immunol* 2016;39:1-6.
[PUBMED](#) | [CROSSREF](#)
15. Jablonska J, Leschner S, Westphal K, Lienenklaus S, Weiss S. Neutrophils responsive to endogenous IFN- β regulate tumor angiogenesis and growth in a mouse tumor model. *J Clin Invest* 2010;120:1151-64.
[PUBMED](#) | [CROSSREF](#)
16. Zhang N, Kim SH, Gainullina A, Erlich EC, Onufer EJ, Kim J, et al. LYVE1+ macrophages of murine peritoneal mesothelium promote omentum-independent ovarian tumor growth. *J Exp Med* 2021;218:e20210924.
[PUBMED](#) | [CROSSREF](#)
17. The Human Protein Atlas. IL34 protein expression summary [Internet]. Stockholm: Knut and Alice Wallenberg Foundation; c2022 [cited 2022 Oct 2]. Available from: <https://www.proteinatlas.org/ENSG00000157368-IL34>.
18. Otsuka R, Wada H, Seino KI. IL-34, the rationale for its expression in physiological and pathological conditions. *Semin Immunol* 2021;54:101517.
[PUBMED](#) | [CROSSREF](#)
19. Kajihara N, Kitagawa F, Kobayashi T, Wada H, Otsuka R, Seino KI. Interleukin-34 contributes to poor prognosis in triple-negative breast cancer. *Breast Cancer* 2020;27:1198-204.
[PUBMED](#) | [CROSSREF](#)
20. Toh M, Ngeow J. Homologous recombination deficiency: cancer predispositions and treatment implications. *Oncologist* 2021;26:e1526-37.
[PUBMED](#) | [CROSSREF](#)
21. Westphalen CB, Fine AD, André F, Ganesan S, Heinemann V, Rouleau E, et al. Pan-cancer analysis of homologous recombination repair-associated gene alterations and genome-wide loss-of-heterozygosity score. *Clin Cancer Res* 2022;28:1412-21.
[PUBMED](#) | [CROSSREF](#)
22. Lee EK, Konstantinopoulos PA. PARP inhibition and immune modulation: scientific rationale and perspectives for the treatment of gynecologic cancers. *Ther Adv Med Oncol* 2020;12:1758835920944116.
[PUBMED](#) | [CROSSREF](#)
23. Fu C, Jiang A. Dendritic cells and CD8 T cell immunity in tumor microenvironment. *Front Immunol* 2018;9:3059.
[PUBMED](#) | [CROSSREF](#)
24. Baghdadi M, Wada H, Nakanishi S, Abe H, Han N, Putra WE, et al. Chemotherapy-induced IL34 enhances immunosuppression by tumor-associated macrophages and mediates survival of chemoresistant lung cancer cells. *Cancer Res* 2016;76:6030-42.
[PUBMED](#) | [CROSSREF](#)
25. Zhou J, Sun X, Zhang J, Yang Y, Chen D, Cao J. IL-34 regulates IL-6 and IL-8 production in human lung fibroblasts via MAPK, PI3K-Akt, JAK and NF- κ B signaling pathways. *Int Immunopharmacol* 2018;61:119-25.
[PUBMED](#) | [CROSSREF](#)

26. Endo H, Hama N, Baghdadi M, Ishikawa K, Otsuka R, Wada H, et al. Interleukin-34 expression in ovarian cancer: a possible correlation with disease progression. *Int Immunol* 2020;32:175-86.
[PUBMED](#) | [CROSSREF](#)
27. Buckley NE, Haddock P, De Matos Simoes R, Parkes E, Irwin G, Emmert-Streib F, et al. A BRCA1 deficient, NFκB driven immune signal predicts good outcome in triple negative breast cancer. *Oncotarget* 2016;7:19884-96.
[PUBMED](#) | [CROSSREF](#)
28. Ding L, Kim HJ, Wang Q, Kearns M, Jiang T, Ohlson CE, et al. PARP inhibition elicits STING-dependent antitumor immunity in Brca1-deficient ovarian cancer. *Cell Reports* 2018;25:2972-2980.e5.
[PUBMED](#) | [CROSSREF](#)
29. Dorner BG, Dorner MB, Zhou X, Opitz C, Mora A, Güttler S, et al. Selective expression of the chemokine receptor XCR1 on cross-presenting dendritic cells determines cooperation with CD8⁺ T cells. *Immunity* 2009;31:823-33.
[PUBMED](#) | [CROSSREF](#)
30. Eisenthal A, Polyvkin N, Bramante-Schreiber L, Misonznik F, Hassner A, Lifschitz-Mercer B. Expression of dendritic cells in ovarian tumors correlates with clinical outcome in patients with ovarian cancer. *Hum Pathol* 2001;32:803-7.
[PUBMED](#) | [CROSSREF](#)
31. Barry KC, Hsu J, Broz ML, Cueto FJ, Binnewies M, Combes AJ, et al. A natural killer-dendritic cell axis defines checkpoint therapy-responsive tumor microenvironments. *Nat Med* 2018;24:1178-91.
[PUBMED](#) | [CROSSREF](#)
32. Böttcher JP, Bonavita E, Chakravarty P, Brees H, Cabeza-Cabrero M, Sammicheli S, et al. NK cells stimulate recruitment of cDC1 into the tumor microenvironment promoting cancer immune control. *Cell* 2018;172:1022-1037.e14.
[PUBMED](#) | [CROSSREF](#)
33. Tang M, Diao J, Gu H, Khatri I, Zhao J, Catral MS. Toll-like receptor 2 activation promotes tumor dendritic cell dysfunction by regulating IL-6 and IL-10 receptor signaling. *Cell Reports* 2015;13:2851-64.
[PUBMED](#) | [CROSSREF](#)
34. Kitamura H, Ohno Y, Toyoshima Y, Ohtake J, Homma S, Kawamura H, et al. Interleukin-6/STAT3 signaling as a promising target to improve the efficacy of cancer immunotherapy. *Cancer Sci* 2017;108:1947-52.
[PUBMED](#) | [CROSSREF](#)
35. Zitvogel L, Galluzzi L, Kepp O, Smyth MJ, Kroemer G. Type I interferons in anticancer immunity. *Nat Rev Immunol* 2015;15:405-14.
[PUBMED](#) | [CROSSREF](#)
36. Martincuks A, Song J, Kohut A, Zhang C, Li YJ, Zhao Q, et al. PARP inhibition activates STAT3 in both tumor and immune cells underlying therapy resistance and immunosuppression in ovarian cancer. *Front Oncol* 2021;11:724104.
[PUBMED](#) | [CROSSREF](#)
37. Jaspers JE, Sol W, Kersbergen A, Schlicker A, Guyader C, Xu G, et al. BRCA2-deficient sarcomatoid mammary tumors exhibit multidrug resistance. *Cancer Res* 2015;75:732-41.
[PUBMED](#) | [CROSSREF](#)
38. Pettitt SJ, Krastev DB, Brandsma I, Dréan A, Song F, Aleksandrov R, et al. Genome-wide and high-density CRISPR-Cas9 screens identify point mutations in PARP1 causing PARP inhibitor resistance. *Nat Commun* 2018;9:1849.
[PUBMED](#) | [CROSSREF](#)
39. Sakai W, Swisher EM, Karlan BY, Agarwal MK, Higgins J, Friedman C, et al. Secondary mutations as a mechanism of cisplatin resistance in BRCA2-mutated cancers. *Nature* 2008;451:1116-20.
[PUBMED](#) | [CROSSREF](#)
40. Ray Chaudhuri A, Callen E, Ding X, Gogola E, Duarte AA, Lee JE, et al. Replication fork stability confers chemoresistance in BRCA-deficient cells. *Nature* 2016;535:382-7.
[PUBMED](#) | [CROSSREF](#)